A thermostable triple mutant of pyranose 2-oxidase from Trametes multicolor with improved properties for biotechnological applications

Oliver Spadiut, Katrin Radakovits, Ines Pisanelli, Clara Salaheddin, Montarop Yamabhai, Tien-Chye Tan, Christina Divne, Dietmar Haltrich

Biotechnology Journal

A thermostable triple mutant of pyranose 2-oxidase from Trametes multicolor with improved properties for biotechnological applications

Journal:	*Biotechnology Journal*
Manuscript ID:	BIOT-2008-0260.R2
Wiley - Manuscript type:	Research Article
Date Submitted by the Author:	28-Nov-2008
Complete List of Authors:	Spadiut, Oliver; Universität für Bodenkultur, Food Sciences and Technology Radakovits, Katrin; Universität für Bodenkultur, Food Sciences and Technology Pisanelli, Ines; Universität für Bodenkultur, Food Sciences and Technology Salaheddin, Clara; Universität für Bodenkultur, Food Sciences and Technology Yamabhai, Montarop; Suranaree University of Technology, School of Biotechnology Tan, Tien-Chye; Royal Institute of Technology KTH, School of Biotechnology Divne, Christina; Royal Institute of Technology KTH, School of Biotechnology Haltrich, Dietmar; Universität für Bodenkultur, Food Sciences and Technology
Keywords:	rational protein design, enzyme engineering, flavoprotein, thermal stability

((5941 words))

Research Article

A thermostable triple mutant of pyranose 2-oxidase from *Trametes multicolor* with improved properties for biotechnological applications

Oliver Spadiut[1], Katrin Radakovits[1], Ines Pisanelli[1], Clara Salaheddin[1], Montarop Yamabhai[2], Tien-Chye Tan[3], Christina Divne[3] & Dietmar Haltrich[1,4*]

[1] Department of Food Sciences and Technology, BOKU - University of Natural Resources and Applied Life Sciences, A-1190 Vienna, Austria

[2] School of Biotechnology, Suranaree University of Technology, Nakhon Ratchasima 30000, Thailand

[3] School of Biotechnology, KTH, Albanova University Centre, SE-106 91 Stockholm, Sweden

[4] Vienna Institute of BioTechnology VIBT, A-1190 Vienna, Austria

*to whom correspondence should be addressed at:

Abteilung für Lebensmittelbiotechnologie, Universität für Bodenkultur, Muthgasse 18, A-1190 Wien, Austria

dietmar.haltrich@boku.ac.at, tel.: +43-1-36006-6275, fax +43-1-36006-6251

Abstract

In order to increase the thermal stability and the catalytic properties of pyranose oxidase (P2Ox) from *Trametes multicolor* towards its poor substrate D-galactose and

the alternative electron acceptor 1,4-benzoquinone (1,4-BQ), we designed the triple-mutant T169G/E542K/V546C. Whereas the wild-type enzyme clearly favors D-glucose as its substrate over D-galactose [substrate selectivity $(k_{cat}/K_M)_{Glc}$ / $(k_{cat}/K_M)_{Gal}$ = 172], the variant oxidizes both sugars equally well [$(k_{cat}/K_M)_{Glc}$ / $(k_{cat}/K_M)_{Gal}$ = 0.69], which is of interest for food biotechnology. Furthermore, the variant showed lower K_M values and approx. tenfold higher k_{cat} values for 1,4-BQ when D-galactose was used as the saturating sugar substrate, which makes this enzyme particularly attractive for use in biofuel cells and enzyme-based biosensors. In addition to the altered substrate specificity and reactivity, this mutant also shows significantly improved thermal stability. The half-life time at 60°C was approximately 10 hrs, compared to 7.6 minutes for the wild-type enzyme. We performed successfully small-scale bioreactor pilot conversion experiments of D-glucose/D-galactose mixtures at both 30°C and 50°C, showing the usefulness of this P2Ox variant in biocatalysis as well as the enhanced thermal stability of the enzyme. Moreover, we determined the crystal structure of the mutant in its unligated form at 1.55 Å resolution. Modeling D-galactose in position for oxidation at C2 into the mutant active site shows that substituting Thr for Gly at position 169 favorably accommodates the axial C4 hydroxyl group that would otherwise clash with Thr169 in the wild-type.

Keywords: flavoprotein; rational protein design; enzyme engineering; thermal stability; biofuel cell; enzymatic batch conversion

1 Introduction

Pyranose 2-oxidase (P2Ox; pyranose:oxygen 2-oxidoreductase; glucose 2-oxidase; EC 1.1.3.10), a flavoprotein found widespread in wood-degrading basidiomycetes, catalyzes the oxidation of different aldopyranoses at C2 to the corresponding 2-ketoaldoses, producing H_2O_2 as a by-product [1–3]. It is a homotetrameric enzyme, typically of a molecular mass of ~270 kDa with each of the four 68-kDa subunits carrying one flavin adenine dinucleotide (FAD) covalently bound [4]. The crystal structure of P2Ox from *Trametes multicolor* was determined at 1.8 Å resolution [5]. An intriguing structural feature of P2Ox is its large internal cavity, from which the active sites are accessible. Four solvent channels lead from the surface of the polypeptide into this cavity through which substrates must enter before accessing the narrow active-site channels of P2Ox. The monosaccharide D-glucose is its preferred substrate and it shows high activities with e.g. D-xylose and L-sorbose, whereas D-galactose is a rather poor substrate with only 5.7% relative activity [6]. Oxidation of D-galactose at position C2 is interesting from an applied point of view, since 2-keto-D-galactose can be easily reduced at position C1 to yield D-tagatose [7], which is used as a non-cariogenic, low caloric sweetener in food industry. Lactose, which is

available in large amounts as a by-product of the cheese and dairy industry, can be hydrolyzed enzymatically, and thus provides an amply supply of D-glucose and D-galactose. For effective biotechnological applications, the catalytic activity of P2Ox with D-galactose, however, is too low, leading to either very long conversion times or disproportionate amounts of required enzyme. Additionally, a conversion at elevated temperatures is desirable, as catalytic activities increase with higher temperatures and also undesired microbiological growth is avoided during conversions at increased temperatures. Besides applications in food industry, P2Ox is becoming attractive for enzymatic biosensors and biofuel cells. Biofuel cells convert sugars into electrical energy by employing oxidoreductases as an anodic biocomponent, and coupling this with a suitable enzyme on the cathode [8]. In mediated electron transfer, certain mediators such as quinones [9] or osmium redox polymers [10] collect the electrons from the prosthetic group of the enzymes and transfer them to a graphite electrode. To improve the performance of biofuel cells it is crucial to increase both the catalytic activity and the stability of the enzymes applied. Rational protein design to change substrate specificity and reactivity has already been successfully performed for oxidoreductases, hydrolases and transferases [11], and thus provides an excellent tool for adapting P2Ox to the above-mentioned biotechnological applications. In order to improve P2Ox from *Trametes multicolor* with respect to its catalytic activity with the poor substrate D-galactose and the alternative electron acceptor 1,4-benzoquinone as well as thermal stability, we combined different mutations, which had previously shown positive effects with respect to the properties of the respective single mutants [12–14]. The mutation E542K, which is located on the surface of the internal cavity, was found to

kinetically stabilize the enzyme as well as to improve its catalytic properties to some extent [12]. Furthermore, Thr169 is thought to affect substrate specificity of P2Ox to some extent. D-Galactose differs from D-glucose by having the C-4 hydroxyl group in axial position rather than equatorial. As described elsewhere, we presume that the axial C-4 hydroxyl group of D-galactose appears sterically hindered by the side chain of Thr169. The replacement of Thr by Gly creates additional space in the active site so that the sugar substrates can be accommodated more easily, resulting in lowered K_M values for D-galactose [14].

Here we report on the detailed biochemical and structural characterization of the resulting P2Ox variant T169G/E542K/V546C, and its possible application for the conversion of D-glucose/D-galactose mixtures at elevated temperatures. To examine the details of the structural effects of the amino-acid substitutions, we also determined the crystal structure of T169G/E542K/V546C in the absence of a ligand at 1.55 Å resolution.

2 Material and methods

2.1 Plasmids, microorganism and media

The construction of the pET21d$^+$/P2Ox vector (pHL2), which expresses the His-tagged pyranose 2-oxidase gene from *Trametes multicolor* under control of the T7 promoter, has been described previously [15]. Active, recombinant wild-type P2Ox and the mutant T169G/E542K/V546C were expressed in the *E. coli* strain BL21 Star DE3 (Invitrogen; Carlsbad, CA, USA). TB_{amp}-medium (yeast extract 24 g/L, peptone from casein 12 g/L, glycerol 4 mL/L; KH_2PO_4-buffer 1 M, pH 7.5) was used for cultivation and protein expression under appropriate selective conditions

(ampicillin was added to 0.1 g/L). All chemicals used were from Sigma (Vienna, Austria) and were of the highest grade available.

2.2 Generation of mutants

The P2Ox gene was mutated by site-directed mutagenesis using PCR and digestion with *Dpn*I [16]. The plasmid pHL2 as template and primers T169G_fwd (5'-gtcgtcgggggcatgtctacgcacctggggatgcgccacacc-3'), T169Grev (5'-ccagtgcgcgcagcagcctccgtacagatgcgtgacc-3'), E542K_V546C_fwd (5'-gaagcctggtctttgccttcaccttggtgg-3') and E542K_V546C_rev (5'-aagaccaggcttcatgaattgcgggagg-3') were used for mutagenic PCRs. The triple mutant T169G/E542K/V546C was generated by sequential mutagenic PCR steps. The PCR reaction mix contained 2.5 U *Pfu* DNA polymerase (Fermentas; St. Leon-Rot, Germany), 100 ng of plasmid DNA, 5 pmol of each primer, 10 µM of each dNTP and 1× PCR buffer (Fermentas) in a total volume of 50 µL. The following conditions were used for mutagenic PCRs: 95°C for 4 min, then 30 cycles of 94°C for 30 s; 56°C for 30 s; 72°C for 16 min, with a final incubation at 72°C for 10 min. After PCR, the methylated template-DNA was degraded by digestion with 10 U of *Dpn*I at 37°C for 3 h. The remaining PCR products were separated by agarose gel electrophoresis and purified using the Wizard SV Gel and PCR-Clean-Up System (Promega; Madison, WI, USA). PCR products (5 µL) were transformed into electro-competent *E. coli* BL21 Star DE3 cells. To prove that only the desired mutations had occurred, the P2Ox-encoding gene was sequenced using primers T7promfwd (5´-aatacgactcactataggg–3´) and T7termrev (5´-gctagttattgctcagcgg-3´).

2.3 Protein expression and purification

Cultures (2 liters) of *E. coli* BL21 Star DE3 transformants were grown in TB_{amp} in shaken flasks at 37°C and 160 rpm. Protein expression was induced at an OD_{600} of ~0.5 by adding lactose to a final concentration of 0.5% (w/v). After incubation at 25°C for further 20 h, approximately 20 g of wet biomass per liter were harvested by centrifugation at 10,000×g for 20 min and 4°C, and resuspended in KH_2PO_4-buffer (50 mM, pH 6.5) containing the protease inhibitor PMSF (0.1% w/v). After disruption in a continuous homogenizer (APV Systems; Silkeborg, Denmark) the crude cell extract was separated from cell debris by centrifugation (70,400×g, 4°C) and used for protein purification by immobilized metal affinity chromatography (IMAC) with a 10-mL BioRad Profinity IMAC Ni-Charged Resin (Biorad; Vienna, Austria). The column was equilibrated with 10 column volumes (CV) of buffer (0.05 M KH_2PO_4, pH 6.5, 0.5 M NaCl, 20 mM imidazole). After the protein sample had been applied to the column it was washed with 3 CV of the same buffer, before proteins were eluted with a linear gradient of 10 CV starting buffer from 20 to 1000 mM imidazole. Active fractions were combined and imidazole was removed by ultrafiltration using an Amicon Ultra Centrifugal Filter Device (Millipore; Billerica, MA, USA) with a 10-kDa cut-off membrane. The concentrated enzymes were washed 3 times with 10 mL of KH_2PO_4-buffer (50 mM, pH 6.5) and finally diluted in the same buffer to a protein concentration of 5–10 mg/mL.

2.4 Enzyme activity assay

P2Ox activity was measured with the standard chromogenic ABTS [2,2'-azinobis(3-ethylbenzthiazolinesulfonic acid)] assay [6]. A sample of diluted enzyme (10 µL) was added to 980 µL of assay buffer containing horseradish peroxidase (142 U),

ABTS (14.7 mg) and KH_2PO_4-buffer (50 mM, pH 6.5). The reaction was started by adding D-glucose (20 mM). The absorbance change at 420 nm was recorded at 30°C for 180 s. The molar absorption coefficient at 420 nm (ε_{420}) used was 42.3 $mM^{-1} \cdot cm^{-1}$. One unit of P2Ox activity was defined as the amount of enzyme necessary for the oxidation of 2 µmol of ABTS per min, corresponding to the consumption of 1 µmol of O_2 per min, under assay conditions. Protein concentrations were determined by the Bradford assay [17] using the BioRad Protein Assay Kit with BSA as standard.

2.5 Steady-state kinetic measurements

Kinetic constants were calculated by non-linear least-squares regression, fitting the data to the Henri-Michaelis-Menten equation. The catalytic constants were measured for the electron donor substrates D-glucose (0.1–50 mM) and D-galactose (0.1–200 mM) using the standard ABTS assay and air saturation. Additionally, catalytic constants were measured for the alternative electron acceptor of this oxidase, 1,4-benzoquinone (1,4-BQ), with 100 mM of either D-glucose or D-galactose as saturating substrate by adding 10 µL of diluted enzyme to 990 µL of assay buffer containing either of the two sugar substrates, KH_2PO_4-buffer (50 mM, pH 6.5) and 1,4-BQ (0.01–2 mM). The absorbance change at 290 nm was recorded at 30°C for 180 s. The chromophore ε_{290} used was 2.24 $mM^{-1} \cdot cm^{-1}$. Steady-state kinetics measurements were carried out both at 30°C and 50°C.

2.6 Electrophoresis

To check the purity of the purified P2Ox variants, electrophoresis was performed as described by Laemmli *et al.* [18]. SDS-PAGE was performed using a 5% stacking gel and a 10% separating gel. The system used was the PerfectBlue vertical

electrophoresis apparatus (Peqlab; Erlangen, Germany). The mass standard used was the Precision Plus Protein Dual Color (Biorad). Gels were stained with Coomassie blue.

2.7 Kinetic stability

Kinetic stability, as expressed by the half-life time of thermal inactivation $\tau_{1/2}$, of the purified wild-type enzyme and the triple mutant was determined by incubating the proteins in appropriate dilutions in 50 mM KH_2PO_4-buffer (pH 6.5) at both 60°C and 70°C for various time intervals and by subsequent measurements of the residual enzyme activity using the standard ABTS assay and D-glucose as substrate. A thermal cycler (thermocycler T3, Biometra; Göttingen, Germany) and thin-walled PCR tubes were used for all thermostability measurements. Residual activities were plotted versus the incubation time and the half-life values of thermal inactivation ($\tau_{1/2}$) were calculated using $\tau_{1/2} = \ln 2/k_{in}$, where k_{in} is the observed rate of inactivation.

2.8 Batch conversion experiments

Wild-type P2Ox and the variant T169G/E542K/V546C were compared in terms of their ability to oxidize D-glucose and D-galactose to the corresponding 2-ketoaldoses with oxygen as electron acceptor at both 30°C and 50°C. Four batch conversion experiments (each with a volume of 300 mL) using equimolar amounts of D-glucose and D-galactose were designed in a way to guarantee a complete conversion of D-galactose within 20 hours for the mutated enzyme and a complete conversion of D-glucose for the wild-type enzyme within reasonable times. The experiments were performed in parallel in a multifermenter (Infors; Bottmingen, Switzerland); these

were initial bioreactor studies proving the applicability of the enzyme variant developed and not aiming at process optimization. The conversion experiments were conducted in 100 mM KH_2PO_4-buffer (pH 6.5) at 400 rpm, a DO_2 concentration of 15%, both at 30°C and 50°C. Catalase was used in excess (100,000 U) to decompose H_2O_2. Depending on the catalytic activity of the enzymes with D-galactose, different amounts of an equimolar mixture of the sugar substrates and biocatalyst concentrations were used for the conversion experiments. For batch conversions (total volume of 300 mL) at 30°C 1600 mU wild-type P2Ox and 400 mU mutated enzyme (measured under standard assay conditions with D-galactose as substrate) were used. The kinetic characterization of the enzymes at 50°C revealed a specific activity of wild-type P2Ox with D-galactose of 500 $mU \cdot mg^{-1}$, of variant T169G/E542K/V546C with 20.4 $mU \cdot mg^{-1}$. Conversions at 50°C were conducted with 2400 mU of wild-type and 750 mU T169G/E542K/V546C, respectively. Samples (2 mL) from the bioconversion experiments were taken periodically, held at 95°C for 5 min to inactivate the enzymes and centrifuged. The supernatants were analyzed for their sugar content using high performance anion exchange chromatography with pulsed amperometric detection (HPAEC-PAD), which was carried out using a Dionex DX-500 system (Dionex; Sunnyvale, CA, USA) and a CarboPac PA-1 column (4 × 250 mm) at 27°C [19].

2.9 X-ray crystallographic analysis

Crystals of the P2Ox variant T169G/E542K/V546C were produced using the hanging drop vapor diffusion method [20]. Drops were prepared by equal volumes of 5 mg/mL protein and reservoir [10% (w/v) monomethylether polyethylene glycol

2000 (mme PEG), 0.1 M Mes (pH 5.2), 50 mM $MgCl_2$, 25% glycerol]. Prior to data collection, the crystals were stabilized using their respective reservoir solution where the PEG concentration had been increased to 50% (stabilizing solution) followed by vitrification in liquid nitrogen. The protein crystallizes in space group $P4_22_12$ with one molecule in the asymmetric unit. Data were collected using synchrotron radiation at MAX-lab (Lund, Sweden), beamline *I*911-3 (λ=1.0 Å; 100 K). Data were processed using *XDS* [21]. Phases for the T169G/E542K/V546C structure were obtained by means of Fourier synthesis using the refined model of P2Ox variant H167A as starting model (PDB code 2IGO; [15]. Crystallographic refinement was performed with *REFMAC5* [22], including anisotropic scaling, calculated hydrogen scattering from riding hydrogens, and atomic displacement parameter refinement using the translation, libration, screw-rotation (TLS) model. The TLS models were determined using the TLS Motion Determination server (TLSMD; [23]). Corrections of the models were done manually based on σ_A-weighted $2F_o$-F_c and F_o-F_c electron density maps. The R_{free} reflection sets were kept throughout refinement. All model building was performed with the program *O* [24] and *Coot* [25]. Data collection and model refinement statistics are given in Table 5. Structural data are available in the Protein Data Base under the accession number 3FDY.

3 Results

3.1 Generation of mutants

After site-directed mutagenesis was performed as described in the Material and Methods section, the presence of the correct and the absence of undesired mutations in the P2Ox gene were confirmed by DNA sequence analysis. Wild-type P2Ox and the variant T169G/E542K/V546C were expressed in *E. coli*, purified to apparent homogeneity and concentrated by ultrafiltration. The purity of the resulting enzyme preparations was confirmed by SDS-PAGE (Fig. 1). Routinely, approx. 20 mg of P2Ox protein were obtained per liter culture medium by this procedure.

3.2 Kinetic characterization

For determination of the steady-state kinetic constants, initial rates of substrate turnover were recorded over a substrate range of 0.1–50 mM D-glucose and 0.1–200 mM D-galactose for wild-type P2Ox and the mutational variant T169G/E542K/V546C using the standard ABTS assay and oxygen (air saturation), both at 30°C and 50°C. Kinetic data are summarized in Table 1. Prior to determination of the kinetic constants it was confirmed that the introduction of the amino acid substitutions in the triple-mutant did not affect the pH profile of P2Ox activity (data not shown). T169G/E542K/V546C showed an approx. 5-fold decreased Michaelis constant K_M for D-galactose compared to the wild-type enzyme when air oxygen was the electron acceptor, whereas K_M for D-glucose was hardly altered. Yet, turnover numbers k_{cat} for both sugar substrates were decreased considerably as well, regardless of the temperature used for activity measurements. As a result, the catalytic efficiency k_{cat}/K_M of the mutant was similar to that of the wild-type enzyme with D-galactose but was decreased ≈400-fold with D-glucose, resulting in an enzyme that showed an equal or even higher k_{cat}/K_M value for D-

galactose than for D-glucose. In contrast, the wild-type enzyme clearly prefers D-glucose over D-galactose as its sugar substrate as is also expressed by the substrate selectivity values, i.e., the ratio of the catalytic efficiencies k_{cat}/K_M for the two substrates. This value is 172 for the wild-type, while it is 0.69 for T169G/E542K/V546C at 30°C.

In addition, the kinetic constants were determined for the alternative electron acceptor 1,4-benzoquinone (1,4-BQ) with either D-glucose or D-galactose in saturating concentrations at 30°C and 50°C (Table 2), and it was found that the three amino acid substitutions dramatically affect the catalytic properties. The K_M value of the mutant for 1,4-BQ was reduced two to three times compared to the wild-type enzyme, regardless of the sugar substrate used. While the turnover number with D-glucose as saturating substrate was reduced significantly, it increased considerably with D-galactose (≈10-fold). Compared to the wild-type enzyme, mutant T169G/E542K/V546C showed a 24- and 15-fold increase in its catalytic efficiency at 30°C and 50°C, respectively, for 1,4-BQ and D-galactose as saturating substrate.

3.3 Thermal stability

Kinetic stability (the length of the time in which an enzyme remains active before undergoing irreversible inactivation) of wtP2Ox and of variant T169G/E542K/V546C was determined at 60°C and at 70°C and a constant pH of 6.5. The inactivation constants k_{in} and the half-lives of denaturation $\tau_{1/2}$ were determined (Table 3), and both enzymes showed first-order inactivation kinetics when analyzed in the ln(residual activity) versus time plot (Fig. 2). The mutation E542K in combination with T169G and V546C stabilized P2Ox significantly. At

60°C the half-life was increased 76-fold compared to the wild-type enzyme. The effect of the mutations on stability is even more pronounced at 70°C, where $\tau_{1/2}$ was increased 350-fold.

3.4 Enzymatic batch conversion experiments

In order to assess the effects of the selected amino acid substitutions on the biocatalytic performance of P2Ox, batch conversion experiments using equimolar mixtures of D-glucose and D-galactose were performed with oxygen as electron acceptor (Fig. 3). Reaction conditions were chosen to guarantee reasonable process times in each reactor and were not aimed at process optimization; hence different amounts of enzyme and sugar substrates were used (Table 4). The specific activity of P2Ox when using D-galactose as the substrate and measuring at 30°C was 330 $mU \cdot mg^{-1}$ for the wild-type and 12.2 $mU \cdot mg^{-1}$ for variant T169G/E542K/V546C. At 30°C the wild-type enzyme clearly preferred D-glucose compared to D-galactose with a conversion rate of 2.0 $g \cdot L^{-1} \cdot h^{-1}$. Only when D-glucose was oxidized completely, D-galactose was converted at a very low rate of 0.02 $g \cdot L^{-1} \cdot h^{-1}$. In contrast to that, mutant T169G/E542K/V546C showed similar conversion rates of 0.054 and 0.065 $g \cdot L^{-1} \cdot h^{-1}$ for D-glucose and D-galactose. The engineered variant did not prefer either of the sugars as its substrate but converted both of them simultaneously. As is also expressed by the slightly higher k_{cat} for D-galactose, this monosaccharide was converted at a somewhat faster rate than D-glucose. When the conversion experiments were performed at 50°C, the wild-type enzyme oxidized D-glucose initially at a high rate of 8.7 $g \cdot L^{-1} \cdot h^{-1}$ for the first phase of the conversion (up to 45 min). Yet, thermal inactivation of the enzyme resulted in a rapid drop of the

conversion rate over time and P2Ox activity was completely lost after 90 min, as was evident from residual D-glucose left in the reaction mixture and the complete lack of 2-keto-D-galactose. In contrast, variant T169G/E542K/V546C converted both sugar substrates at an almost equal rate of 0.12 $g \cdot L^{-1} \cdot h^{-1}$ resulting in complete conversion of both sugar substrates within 20 h.

4 Discussion

Pyranose oxidase is an enzyme of interest for use in biofuel cells and enzyme-based biosensors as well as for applications in food industry. In several previous studies the improvement of P2Ox both in terms of stability and reactivity was reported. The mutation E542K was found to improve both the kinetic and thermodynamic stability of the enzyme as well as its catalytic properties to some extent [12, 26]. Other studies showed the positive effects of the mutations V546C [13] and T169G [14] with respect to kinetic properties, especially for the oxidation of the substrate D-galactose. The replacement of Val by Cys at position 546 in the direct vicinity of the active site of P2Ox resulted in significantly increased turnover rates for both the sugar substrate and the alternative electron acceptor, albeit at the costs of an increased K_M. We determined the crystal structure of the T169G/E542K/V546C mutant at 1.55 Å resolution and performed theoretical modeling of β-D-glucose and β-D-galactose in the active site (Fig. 4). The axial C4 hydroxyl in β-D-galactose cannot be accommodated easily in the active site and clashes with the side chain of Thr169, whereas the β-D-glucose C4 hydroxyl fits well. In the mutant, Gly169 relieves steric hindrance and provides space for the galactose C4 hydroxyl group to

give a relative decrease in K_M value. This, at least partly, explains why β-D-galactose is a poor substrate for wild-type P2Ox, and performs relatively better as substrate for P2Ox T169G/E542K/V546C. By introducing this mutation we intended to counteract the negative effects on K_M observed for the V546C mutation. By combining these three different mutations we aimed at creating a thermostable variant of P2Ox, which converts D-galactose and D-glucose concomitantly and at equal rates. This simultaneous conversion of D-glucose and D-galactose is important when e.g. lactose hydrolysates are used as a starting material for the envisaged bioconversion. P2Ox is known to overoxidize its primary reaction product, 2-keto-D-glucose, thus forming 2,3-diketo-D-glucose [27]. Simultaneous conversion of the two sugar substrates will obviously avoid this overoxidation and thus the formation of the undesired by-product. We were further interested in increasing the turnover number for 1,4-benzoquinone, which can be used as electron mediator in biofuel cells and biosensors, in combination with D-galactose as the saturating substrate. In biofuel cells based on mediated electron transfer, suitable mediators gather electrons from the prosthetic group of an enzyme and transfer them to the electrode. In these applications, the measured current represents the actual turnover rate of the immobilized enzyme, and, consequently, an enzyme with increased turnover rates for the mediator will boost the power output of biofuel cells [8, 10] or improve enzyme electrodes [30].

Kinetic characterization and comparison of variant T169G/E542K/V546C showed that the substrate selectivity was indeed changed significantly for the mutant. Whereas wtP2Ox clearly prefers D-glucose as its substrate, as indicated by a considerably higher k_{cat}/K_M value, T169G/E542K/V546C does not show any clear

preference for either sugar substrate as is evident from comparable catalytic efficiencies. This change in substrate selectivity, however, comes at a cost in k_{cat}, which is reduced for the triple-mutant for both sugar substrates. The altered sugar selectivity is also obvious when performing small-scale conversion experiments, using equimolar mixtures of D-glucose and D-galactose, as found in lactose hydrolysates, as the starting material.

Here, the variant oxidized both sugars simultaneously, while the wild-type enzyme converted D-galactose only when D-glucose was exhausted from the reaction mixture. Introducing the E542K mutation in the variant also enabled conversions at higher temperatures, which is preferable because of higher reaction rates and a decreased possibility of microbial contamination. The triple-mutant showed considerably increased thermostability as is evident from the remarkable increase in half-life times, at both 60°C and 70°C, which were improved 76-fold and 350-fold, respectively, when compared to the wild-type. Thus, bioconversions based on the thermostable variant will be feasible at temperatures of up to 60°C.

The triple-mutant T169G/E542K/V546C also showed significantly improved catalytic properties for its substrate 1,4-BQ when D-galactose was the saturating sugar. Compared to the wild-type enzyme, the turnover numbers for 1,4-BQ with D-galactose as saturated substrate at 30°C and at 50°C were increased 9-fold and 12-fold, respectively, for the variant. In combination with a lowered K_M value for the electron acceptor the resulting catalytic efficiency was 24 times and 15 times higher, respectively, compared to the wild-type enzyme. This property, together with its considerably increased stability, makes this variant particularly promising for

applications in biofuel cells. The bioelectrochemical properties of T169G/E542K/V546C are currently studied in our laboratory.

Acknowledgements

Financial support from the Austrian Science Fund (Fonds zur Förderung der wissenschaftlichen Forschung, Translational Project L213-B11) to DH is gratefully acknowledged. CD has been supported by grants from the Swedish Research Council for Environment, Agricultural Sciences and Spatial Planning (Formas), the Swedish Research Council, the CF Lundströms Foundation, and the Carl Tryggers Foundation. We thank the beamline staff scientists at MAX-lab (Lund, Sweden) for support during data collection.

The authors have declared no conflict of interest.

5 References

[1] Volc, J., Denisova, N. P., Nerud, F., Musílek, V. Glucose-2-oxidase activity in mycelial cultures of basidiomycetes. *Folia Microbiol.* 1985, *30*, 141–147.

[2] Daniel, G., Volc, J., Kubátová, E. Pyranose oxidase, a major source of H_2O_2 during wood degradation by *Phanerochaete chrysosporium*. *Appl. Environ. Microbiol.* 1994, *60*, 2524–2532.

[3] Leitner, C., Haltrich, D., Nidetzky, B., Prillinger, H., Kulbe, K. D. Production of a novel pyranose 2-oxidase by basidiomycete *Trametes multicolor*. *Appl. Biochem. Biotechnol.* 1998, *70–72*, 237–248.

[4] Halada, P., Leitner, C., Sedmera, P., Haltrich, D., Volc, J. Identification of the covalent flavin adenine dinucleotide-binding region in pyranose 2-oxidase from *Trametes multicolor*. *Anal. Biochem.* 2003, *314*, 235–242.

[5] Hallberg, B. M., Leitner, C., Haltrich, D., Divne, C. Crystal structure of the 270 kDa homotetrameric lignin-degrading enzyme pyranose 2-oxidase. *J. Mol. Biol.* 2004, *341*, 781–796.

[6] Leitner, C., Volc, J., Haltrich, D. Purification and characterization of pyranose oxidase from the white-rot fungus *Trametes multicolor*. *Appl. Environ. Microbiol.* 2001, *67*, 3636–3644.

[7] Haltrich, D., Leitner, C., Neuhauser, W., Nidetzky, B., Kulbe, K. D., Volc, J. A convenient enzymatic procedure for the production of aldose-free D-tagatose. *Anal. NY Acad. Sci.* 1998, *864*, 295–299.

[8] Heller, A. Miniature biofuel cells. *Phys. Chem. Chem. Phys.* 2004, *6*, 209–216.

399 [9] Tamaki, T., Ito, T., Yamaguchi. T. Immobilization of hydroquinone through a
400 spacer to polymer grafted on carbon black for a high-surface-area biofuel cell
401 electrode. *J. Phys. Chem. B.* 2007, *34***,** 1012–1039.
402 [10] Tasca, F., Timur, S., Ludwig, R., Haltrich, D., Volc, J., Antiochia, R., Gorton,
403 L. Amperometric biosensors for detection of sugars based on the electrical wiring of
404 different pyranose oxidases and pyranose dehydrogenases with osmium redox
405 polymer on graphite electrodes. *Electroanalysis* 2007, *19*, 294–302.
406 [11] Penning, T. M., Jez, J. M. Enzyme redesign. *Chem. Rev.* 2001, *101*, 3027–3046.
407 [12] Masuda-Nishimura, I., Minamihara, T., Koyama, Y. Improvement in thermal
408 stability and reactivity of pyranose oxidase from *Coriolus versicolor* by random
409 mutagenesis. *Biotechnol. Lett.* 1999, *21*, 203–207.
410 [13] Salaheddin, C., Spadiut O., Tan, T.-C., Divne, C., Haltrich, D., Peterbauer, C.
411 Probing active-site residues of pyranose 2-oxidase from *Trametes multicolor* by
412 semi-rational protein design. *Biotechnol. J.*, doi 10.1002/biot.200800265.
413 [14] Spadiut, O., Leitner, C., Tan, T.-C., Ludwig, R., Divne, C., Haltrich, D.
414 Mutations of Thr169 affect substrate specificity of pyranose 2-oxidase from
415 *Trametes multicolor*. *Biocatal. Biotrans.* 2008, *26*, 120–127.
416 [15] Kujawa, M., Ebner, H., Leitner, C., Hallberg, B., Prongjit, M., Sucharitakul, J.,
417 Ludwig, R., Rudsander, U., Peterbauer, C., Chaiyen, P., Haltrich, D., Divne, C.
418 Structural basis for substrate binding and regioselective oxidation of
419 monosaccharides at C3 by pyranose 2-oxidase. *J. Biol. Chem.* 2006, *46*, 35104–
420 35115.
421 [16] Li, S., Wilkinson, M. F. Site-directed mutagenesis: a two-step method using
422 PCR and *Dpn*I. *Biotechniques* 1997, *4,* 588–590.

[17] Bradford, M. M. A rapid and sensitive method for the quantitation of microgram quantities of protein utilizing the principle of protein-dye binding. *Anal. Biochem.* 1976, *72*, 248–254.

[18] Laemmli, U. K. Cleavage of structural proteins during the assembly of the head of bacteriophage T4. *Nature* 1970, *227*, 680–685.

[19] Splechtna, B., Nguyen, T.-H., Steinböck, M., Kulbe, K. D., Lorenz, W., Haltrich, D. Production of prebiotic galacto-oligosaccharides from lactose using β-galactosidases from *Lactobacillus reuteri*. *J. Agric. Food Chem.* 2006, *54*, 4999–5006.

[20] McPherson, A. *Preparation and Analysis of Protein Crystals*, John Wiley & Sons, 1982.

[21] Kabsch, W. Automatic processing of rotation diffraction data from crystals of initially unknown symmetry and cell constants. *J. Appl. Cryst.* 1993, *26*, 795–800.

[22] Murshudov, G. N., Vagin, A. A., Dodson E. J. Refinement of macromolecular structures by the maximum-likelihood method. *Acta Crystallogr. Sect. D* 1997, *53*, 240–255.

[23] Painter, J., Merritt, E. A. Optimal description of a protein structure in terms of multiple groups undergoing TLS motion. *Acta Crystallogr. Sect. D* 2006, *62*, 439–450.

[24] Jones, T. A., Zou, J.-Y., Cowan, S. W., Kjeldgaard, M. Improved methods for building protein models in electron density maps and the location of errors in these models. *Acta Crystallogr. Sect. A* 1991, *47*, 110–119.

[25] Emsley, P., Cowtan, K. Coot: model-building tools for molecular graphics. *Acta Crystallogr. Sect. D* 2004, *60*, 2126–2132.

[26] Bastian, S., Rekowski, M. J., Witte, K., Heckmann-Pohl, D. M., Giffhorn, F. Engineering of pyranose 2-oxidase from *Peniophora gigantea* towards improved thermostability and catalytic efficiency. *Appl. Microbiol. Biotechnol*. 2005, *67***,** 654–663.

[27] Giffhorn, F. Fungal pyranose oxidases: occurrence, properties and biotechnical applications in carbohydrate chemistry. *Appl. Microbiol. Biotechnol*. 2000, *54***,** 727–740.

[28] DeLano, W. L. *The PyMOL Molecular Graphics System*, DeLano Scientific, Palo Alto, CA, USA, 2002. http://www.pymol.org.

[29] Lovell, S. C., Davis, I. W., Arendall, W. B. 3rd, de Bakker, P. I., Word, J. M., Prisant, M. G., Richardson, J. S., Richardson, D. C. Structure validation by C-α geometry: ϕ, ψ, and C-β deviation. *Proteins* 2003, *50*, 437–450.

[30] Rabinovich, M. L., Vasil'chenko, L. G., Karapetyan, K. N., Shumakovich, G. P., Yershevich, O. P., Ludwig, R., Haltrich, D., Hadar, Y., Kozlov, Y. P., Yaropolov, A. I. Application of cellulose-based self-assembled tri-enzyme system in a pseudo-reagent-less biosensor for biogenic catecholamine detection. *Biotechnol. J*. 2007, *2*, 546–558.

Legends to figures

Figure 1. SDS-PAGE analysis of purified wild-type P2Ox from *Trametes multicolor* and the mutational variant T169G/E542K/V546C. Lane 1, molecular mass marker proteins; lane 2, wild-type P2Ox; lane 3, T169G/E542K/V546C after purification by IMAC.

Figure 2. Inactivation kinetics of P2Ox variants from *Trametes multicolor* at pH 6.5 and various temperatures. A: wtP2Ox and the variant T169G/E542K/V546C at 60°C; ; B: ●, wild-type P2Ox/variant T169G/E542K/V546C at 70°C, the inset shows the inactivation of the triple mutant. Symbols: ●, wtP2Ox; ■, T169G/E542K/V546C

Figure 3. Batch conversion experiments of equimolar mixtures of D-glucose and D-galactose and oxygen as electron acceptor at both 30°C and 50°C using wild-type *Tm*P2Ox or the variant T169G/E542K/V546C as biocatalyst.
A, wtP2Ox at 30°C; B, T169G/E542K/V546C at 30°C; C, wtP2Ox at 50°C; D, T169G/E542K/V546C at 50°C. Symbols: ●, D-glucose; ▲, D-galactose

Figure 4. Theoretical models showing the presumed binding of a) *β*-D-glucose, and b) *β*-D-galactose in the active site of *T. multicolor* P2Ox variant T169G/E542K/V546C based on the crystal structure of P2Ox variant H167A in complex with 2-fluoro-2-deoxy-D-glucose (PDB code 2IGO; [15]). The triple mutant is shown in yellow, and the protein model of 2IGO in light blue (ligand removed). The modeled monosaccharides (glucose and galactose) are shown in light

green. For clarity, protein backbone atoms and water molecules have been omitted. The covalent linkage between the FAD 8α methyl group and His167 $N^{\varepsilon 2}$ is indicated. The monosaccharides are oriented for oxidation at C2, and their C4 atoms are marked by an asterisk (*). Modeling was performed using the program O [24], and the picture was made using MacPyMOL v. 0.98 [28].

Table 1. Steady-state kinetic constants of wild-type P2Ox and variant T169G/E542K/V546C with either D-glucose or D-galactose as substrate and O_2 (air) as electron acceptor at pH 6.5 and at the temperatures indicated.

	30°C			50°C		
D-Glucose	K_M (mM)	k_{cat} (s^{-1})	k_{cat}/K_M ($mM^{-1}\ s^{-1}$)	K_M (mM)	k_{cat} (s^{-1})	k_{cat}/K_M ($mM^{-1}\ s^{-1}$)
wtP2Ox	0.76 ± 0.05	34.0 ± 0.43	44.7	1.18 ± 0.08	58.9 ± 0.93	50.0
T169G/E542K/V546C	0.64 ± 0.10	0.072 ± 0.003	0.11	1.15 ± 0.12	0.35 ± 0.008	0.30
D-Galactose						
wtP2Ox	7.94 ± 0.39	2.10 ± 0.03	0.26	14.6 ± 1.57	5.51 ± 0.16	0.38
T169G/E542K/V546C	1.66 ± 0.70	0.27 ± 0.02	0.16	2.76 ± 0.34	0.74 ± 0.02	0.27

Table 2. Steady-state kinetic constants of wild-type P2Ox and variant T169G/E542K/V546C for 1,4-benzoquinone as electron acceptor with either D-glucose or D-galactose as saturating substrate. Data were determined at pH 6.5 and at the temperatures indicated.

	30°C			50°C		
D-Glucose	K_M (mM)	k_{cat} (s^{-1})	k_{cat}/K_M ($mM^{-1}s^{-1}$)	K_M (mM)	k_{cat} (s^{-1})	k_{cat}/K_M ($mM^{-1}s^{-1}$)
wtP2Ox	0.40 ± 0.05	349 ± 17.8	863	0.78 ± 0.07	615 ± 32.6	785
T169G/E542K/V546C	0.22 ± 0.10	21.16 ± 3.7	94.5	0.31 ± 0.15	79.3 ± 16.6	258
D-Galactose						
wtP2Ox	0.25 ± 0.03	6.61 ± 0.34	26.3	0.23 ± 0.037	14.6 ± 0.69	62.1
T169G/E542K/V546C	0.093 ± 0.04	59.6 ± 7.59	622	0.19 ± 0.084	171 ± 28.2	911

Table 3. Kinetic stability of pyranose oxidase from *T. multicolor* at various temperatures. The inactivation constants k_{in} and half-life times of inactivation $\tau_{1/2}$ are given for 60°C and 70°C.

Variant	60°C		70°C	
	k_{in} (min^{-1})	$\tau_{1/2}$ (min)	k_{in} (min^{-1})	$\tau_{1/2}$ (min)
wtP2Ox	$-9.15 \cdot 10^{-2}$	7.6	–5.57	0.12
T169G/E542K/V546C	$-1.20 \cdot 10^{-3}$	578	$-1.65 \cdot 10^{-2}$	42.0

Table 4. Batch conversion experiments of wild-type pyranose oxidase from *T. multicolor* and the variant T169G/E542K/V546C using equimolar mixtures of D-glucose and D-galactose at 30°C and at 50°C.

	batch A	batch B	batch C	batch D
Enzyme	wild-type	variant	wild-type	variant
Temperature (°C)	30°C	30°C	50°C	50°C
Enzyme activity applied (mU)	1600	400	2400	750
Initial sugar concentration ($g \cdot L^{-1}$)	0.8	0.3	10	0.5
Conversion rate D-glc ($g \cdot L^{-1} \cdot h^{-1}$)	2.0	0.051	8.7 / 2.7[b]	0.117
Conversion rate D-gal ($g \cdot L^{-1} \cdot h^{-1}$)	0.02[a]	0.065	0.00[b]	0.124

[a] D-gal was not converted until D-glc was completely oxidized

[b] during the first 45 min the average conversion rate was high with 8.7 $g \cdot L^{-1} \cdot h^{-1}$, inactivation resulted in a lower average conversion rate of 2.7 $g \cdot L^{-1} \cdot h^{-1}$ over the subsequent 45 min period, wild-type enzyme was completely inactived after 90 minutes

Table 5. Data collection and refinement statistics

Data collection[1]	T169G/E542K/V546C
Cell constants a=b, c (Å); β (°) / Space group	101.58, 126.85
Resolution range, nominal (Å)	79.3-1.55 (1.60-1.55)
Unique reflections	1,581,896 (96,227)
Multiplicity	16.4 (11.3)
Completeness (%)	99.8 (97.5)
$<I / \sigma I>$	12.8 (2.8)
R_{sym}[2] (%)	15.9 (88.5)
Refinement	
Resolution range (Å)	60.0–1.55
Completeness, all % (highest bin)	99.8 (98.4)
R_{factor}[3]/work reflns, all	18.6 / 93,323
R_{free}/free reflns, all	21.9 / 2,899
Non-hydrogen atoms	5,078
Mean *B* (Å^2) protein all/mc/sc	11.5 / 10.5 / 12.6
Mean *B* (Å^2) solvent / N^o. molecules	23.5 / 475
Rmsd bond lengths (Å), angles (°)	0.022, 1.98
Ramachandran: favored / allowed (%)[4]	97.7 / 100

[1] The outer shell statistics of the reflections are given in soft brackets. Shells were selected as defined in *XDS* [21] by the user.

[2] $R_{sym} = [\Sigma_{hkl} \Sigma_i |I - <I>| / \Sigma_{hkl} \Sigma_i |I|] \times 100$ %.

[3] $R_{factor} = \Sigma_{hkl} \mid |F_o| - |F_c| \mid / \Sigma_{hkl} |F_o|$

[4] As determined by *MolProbity* [29]

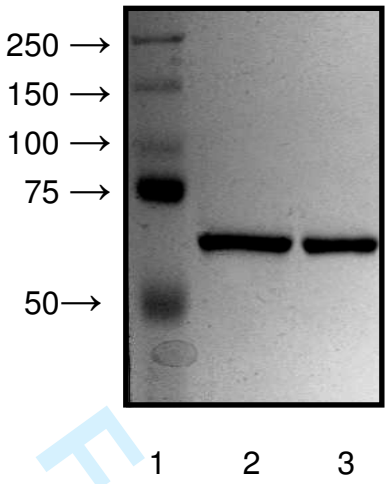

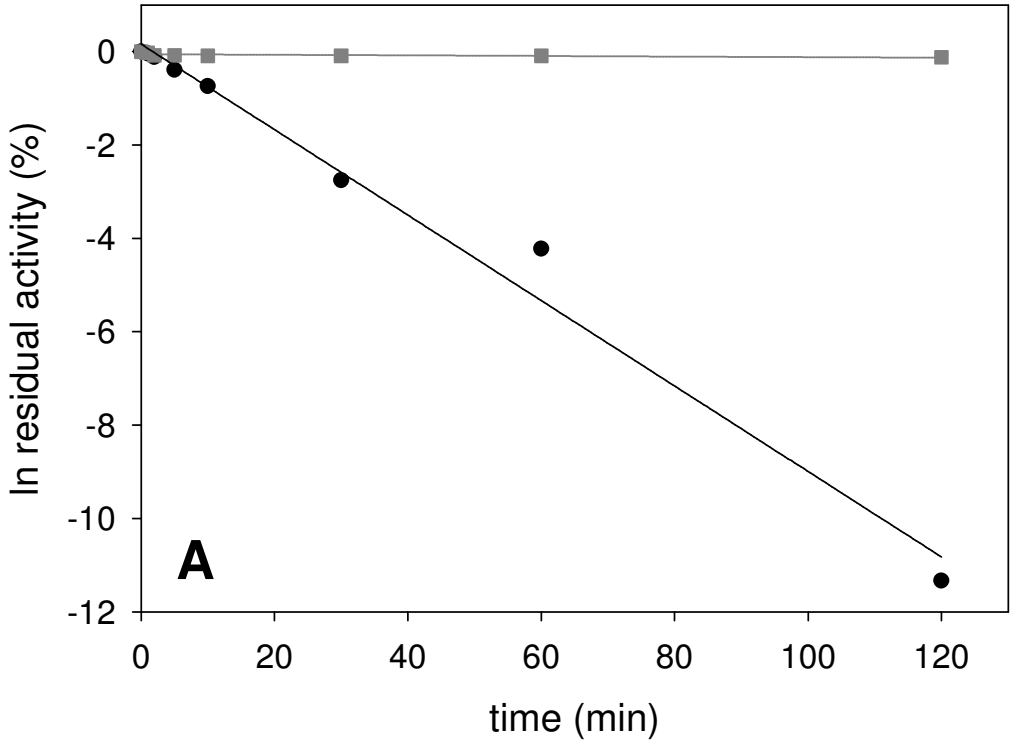
ln residual activity (%)
0
-2
-4
-6
-8
-10
-12
A
0
20
40
60
80
100
120
time (min)

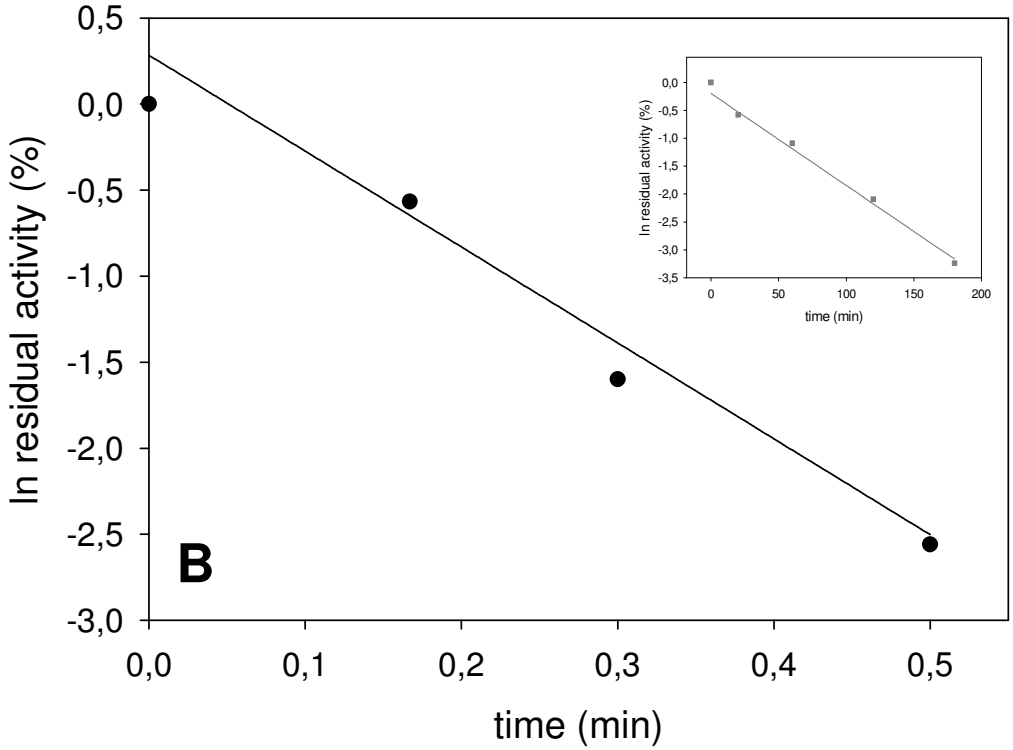
ln residual activity (%)
0,5
0,0
-0,5
-1,0
-1,5
-2,0
-2,5
-3,0
B
0,0
0,1
0,2
0,3
0,4
0,5
time (min)
ln residual activity (%)
0,0
-0,5
-1,0
-1,5
-2,0
-2,5
-3,0
-3,5
0
50
100
150
200
time (min)

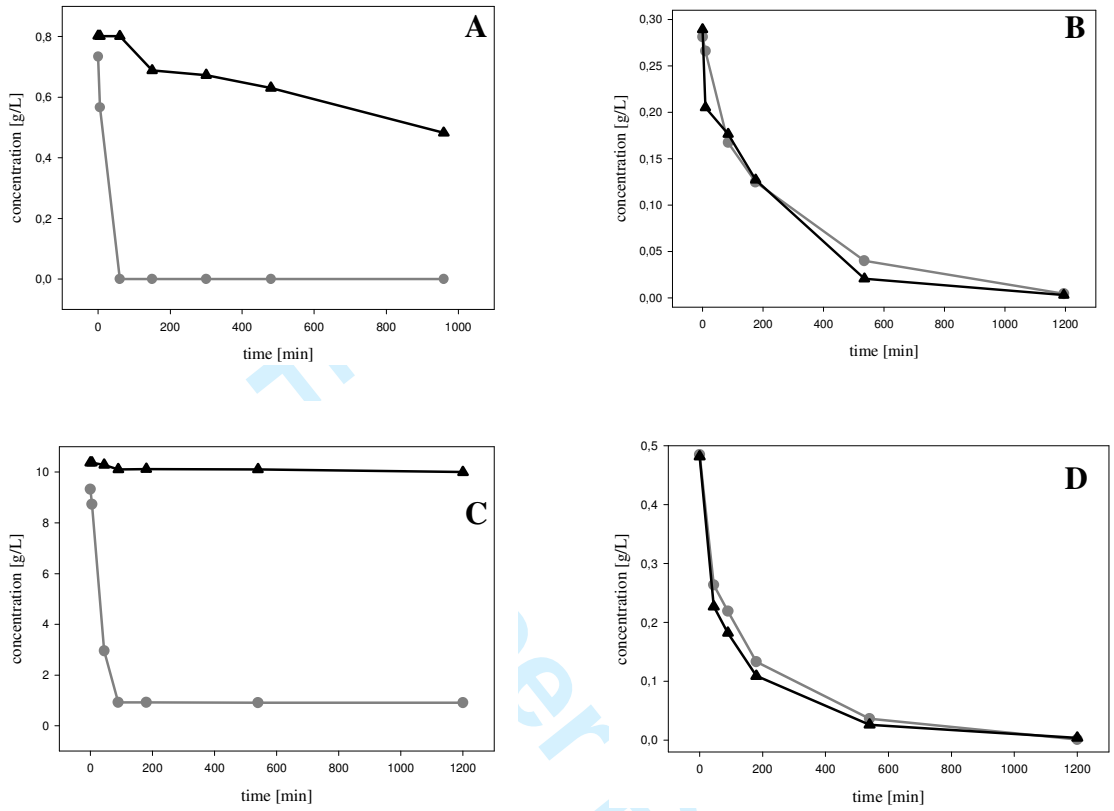

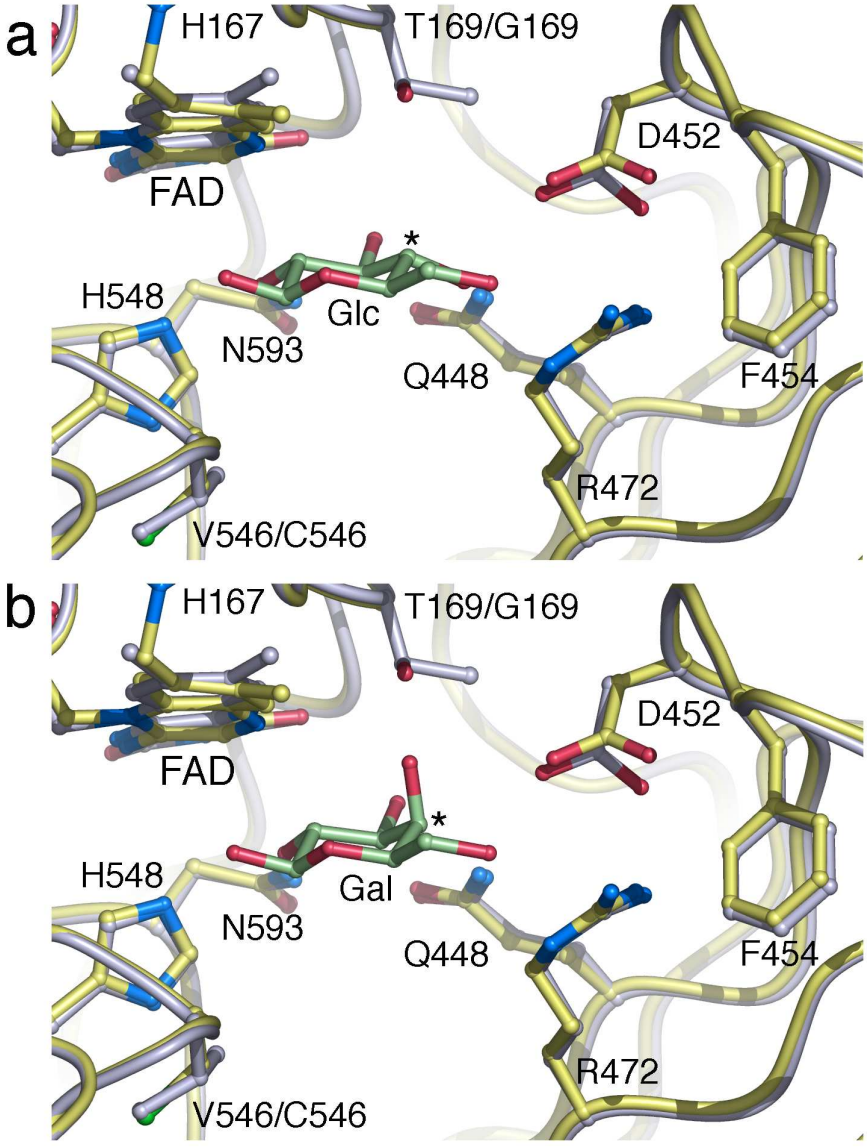

Figure 4
63x84mm (600 x 600 DPI)